Characterisation of an atypical manifestation of black band disease on *Porites lutea* in the Western Indian Ocean

Mathieu Séré, David A Wilkinson, Michael H Schleyer, Pascale Chabanet, Jean-Pascal Quod, Pablo Tortosa

Recent surveys conducted on Reunion Island coral reefs revealed an atypical manifestation of black band disease on the main framework building coral, Porites lutea. This BBD manifestation (PorBBD) presented a thick lighter-colored band, which preceded the typical BBD lesion. Whilst BBD aetiology has been intensively described worldwide, it remains unclear if corals with apparently similar lesions across coral reefs are affected by the same pathogens. Therefore, a multidisciplinary approach involving field surveys, gross lesion monitoring, histopathology and 454-pyrosequencing was employed to provide the first comprehensive characterization of this particular manifestation. Surveys conducted within two geomorphological zones over two consecutive summers and winters showed spatial and seasonal patterns consistent with those found for typical BBD. Genetic analyses suggested an uncharacteristically high level of Vibrio spp. bacterial infection within PorBBD. However, microscopic analysis revealed high densities of cyanobacteria, penetrating the compromised tissue as well as the presence of basophilic bodies resembling bacterial aggregates in the living tissue, adjacent to the bacterial mat. Additionally, classical BBD-associated cyanobacterial strains, genetically related to Pseudoscillatoria coralii and Roseofilum reptotaenium were identified and isolated and the presence of sulfate-reducers or sulfide-oxidizers such as Desulfovibrio and Arcobacter, previously shown to be associated with anoxic microenvironment within typical BBD was also observed, confirming that PorBBD is a manifestation of classical BBD.

1 **Characterisation of an atypical manifestation of black band disease on *Porites***

2 ***lutea* in the Western Indian Ocean**

4 **Mathieu G. Séré[1, 2, 3*], David A Wilkinson[4], Michael H. Schleyer[2], Pascale Chabanet[3], Jean-Pascal**

5 **Quod[1], Pablo Tortosa[4]**

7 **1** ARVAM, 2 rue Maxime Rivière, 97490 Ste Clotilde, Reunion Island, France.

8 **2** Oceanographic Research Institute (ORI), PO Box 10712, Marine Parade, Durban, 4056 South Africa,

9 **3** IRD-UMR ENTROPIE, Labex CORAIL, CS 41095, 97495 Sainte Clotilde Cedex, La Réunion.

10 **4** Unité Mixte de Recherche "Processus Infectieux en Milieu Insulaire Tropical" (UMR PIMIT), Université de La Réunion, Inserm1187,

11 CNRS9192, IRD249, Plateforme de Recherche CYROI, 2 rue Maxime Rivière, 97490 Ste Clotilde, Saint Denis, France.

13 **Abstract**

14 Recent surveys conducted on Reunion Island coral reefs revealed an atypical manifestation of

15 black band disease on the main framework building coral, *Porites lutea*. This BBD manifestation

16 (PorBBD) presented a thick lighter-colored band, which preceded the typical BBD lesion. Whilst

17 BBD aetiology has been intensively described worldwide, it remains unclear if corals with

18 apparently similar lesions across coral reefs are affected by the same pathogens. Therefore, a

19 multidisciplinary approach involving field surveys, gross lesion monitoring, histopathology and

20 454-pyrosequencing was employed to provide the first comprehensive characterization of this

21 particular manifestation. Surveys conducted within two geomorphological zones over two

22 consecutive summers and winters showed spatial and seasonal patterns consistent with those found

23 for typical BBD. Genetic analyses suggested an uncharacteristically high level of *Vibrio* spp.

24 bacterial infection within PorBBD. However, microscopic analysis revealed high densities of

25 cyanobacteria, penetrating the compromised tissue as well as the presence of basophilic bodies

26 resembling bacterial aggregates in the living tissue, adjacent to the bacterial mat. Additionally,

27 classical BBD-associated cyanobacterial strains, genetically related to *Pseudoscillatoria coralii*

28 and *Roseofilum reptotaenium* were identified and isolated and the presence of sulfate-reducers or

29 sulfide-oxidizers such as *Desulfovibrio* and *Arcobacter*, previously shown to be associated with

30 anoxic microenvironment within typical BBD was also observed, confirming that PorBBD is a

31 manifestation of classical BBD.

1. Introduction

Black band disease (BBD) is one of the most widespread (Richardson 2004; Richardson et al. 2009), destructive (Gantar et al. 2011; Richardson et al. 2009; Sato et al. 2009) and intensively studied diseases on coral reefs worldwide (Al-Moghrabi 2001; Boyett 2006; Boyett et al. 2007; Dinsdale 2002; Edmunds 1991; Kuta & Richardson 2002; Raymundo & Weil 2016; Rodriguez & Croquer 2008; Rützler et al. 1983; Sato et al. 2009; Voss & Richardson 2006; Zvuloni et al. 2009). Gross lesions of BBD are generally described (based on their presentation in the field) as a dark-coloured band (a few millimetres to centimetres wide, and up to 1 mm thick) separating living tissue from dead skeleton, and migrating across the coral colony (Antonius 1981; Cooney et al. 2002; Gantar et al. 2011; Myers & Richardson 2009; Raymundo & Weil 2016; Rützler et al. 1983). As many as 70 coral species have been reported to be affected by BBD (Sutherland et al. 2004), particularly massive and slow-growing reef building corals (Gantar et al. 2011; Richardson 2004). Factors affecting susceptibility of corals to BBD or enhancing its progression and spread in corals are still not fully understood (Aeby & Santavy 2006; Boyett et al. 2007; Rodriguez & Croquer 2008; Sato et al. 2009; Voss & Richardson 2006; Zvuloni et al. 2009). However, a few experimental studies have linked nutrient enrichment, elevated temperature and light intensity to the pathogenesis of BBD in corals (Aeby & Santavy 2006; Boyett et al. 2007; Voss & Richardson 2006).

Historically, BBD pathology was first microscopically described as a microbial consortium dominated by filamentous cyanobacteria associated with sulphate reducing (Garrett & Ducklow 1975) and sulphide oxidizing bacteria (Rützler et al. 1983). Later, studies using culture-independent molecular techniques revealed a dense and diverse microbial community classified into four functional groups, comprising photoautotrophs (*Cyanobacteria*), sulphate reducers

59   (*Desulfovibrio*), sulphide oxidizers (*Beggiatoa*) and organo-heterotrophs (*Vibrio*) (Cooney et al.

60   2002; Frias-Lopez et al. 2004; Myers et al. 2007; Richardson 2004; Sekar et al. 2006; Viehman et

61   al. 2006). Among these groups, a few bacteria have been suspected to be primary pathogens,

62   including *Desulfovibrio* spp (Viehman et al. 2006) and *Vibrio coralliilyticus* (Arotsker et al. 2009);

63   however, none of these species have been tested experimentally and/or satisfied Henle Koch's

64   postulates. In addition, variations have been detected in bacterial communities associated with

65   BBD across geographic regions and between sympatric coral species (Voss et al. 2007). For

66   instance, the presence of 16S rDNA sequences similar to *Trichodesmium* and *Oscillatoria* were

67   reported in BBD-infected samples from Papua New-Guinea (Frias-Lopez et al. 2002), whereas

68   members of the genera *Geitlerinema*, *Leptolyngbya*, *Lyngbya*, *Oscillatoria*, *Phormidium*,

69   *Pseudoscillatoria* and *Roseofilum* were detected in BBD from the Caribbean, Philippines and Red

70   sea (Casamatta et al. 2012; Myers et al. 2007; Rasoulouniriana et al. 2009; Sekar et al. 2006). More

71   recently, an early stage of BBD has been identified, named cyanobacterial patch (CP), where

72   bacterial communities are initially rich in *Bennothrix* sp. before being progressively displaced by

73   bacteria related to *Oscillatoria* sp. (Sato et al. 2009; Sato et al. 2010). The high variability in BBD

74   bacterial communities found between localities and infected host species may indicate that BBD

75   actually derives from an earlier infection, which favours the infection and subsequent proliferation

76   of opportunistic microorganisms such as cyanobacteria. However, beyond this highly speculative

77   assumption and despite being intensively studied worldwide, the mechanisms of BBD

78   development remain unclear and no primary pathogens have yet been clearly identified.

79   Recent surveys, conducted on western Indian Ocean (WIO) coral reefs (Fig.1) over two

80   consecutive summers and winters between 2010 and 2012 (Séré et al. 2015), revealed an atypical

81   manifestation of black band disease on two of the main framework building corals, *Porites lobata*

82   and *Porites lutea*, and hereafter referred to as "*Porites* black band disease" (PorBBD). Following

83   standardized terminology (Work & Aeby 2006), PorBBD is characterized by a diffuse, central or

84   peripheral, undulating to smooth, gray to black band, leaving behind dead skeleton (Fig.2). The

85   older exposed skeleton is progressively colonized by endophytic algae. In contrast with typical

86   BBD, PorBBD exhibits a lighter black band and a thin to medium (0.5-2 cm in width), undulating

87   to smooth white band of bleached tissue separating the healthy tissue from the black band itself.

88   Our study aimed at providing a comprehensive characterization of PorBBD using a

89   multidisciplinary approach involving field surveys, gross lesion monitoring, and description of

90   histopathologic features together with a description of the associated bacterial diversity.

2. Material and methods

92

93   The sampling of *Porites lutea* colonies for this study was authorised by the French Department of

94   Ecology, Sustainable Development, Transportation and Housing (DEAL), and CITES (Permit no.

95   FR1197400391-FR1197400394-1)

96   *Field surveys and progression rate*

97   Surveys were undertaken in Reunion at four latitudinal sites on the outer reef slope and reef flat

98   following protocols adapted to these geomorphological zones. The outer reef slope is characterized

99   by a succession of spurs and grooves that represent different habitats. Spurs are covered mainly

100   with hard corals, whereas grooves are often filled with sand and coral rubble. In order to stay

101   within the coral community, five 10 m x 2 m belt-transects were laid along the different spurs at

102   the same depth. Surveys on the inner reef flat were conducted along three 20 m x 2 m belt-transects

103   positioned parallel to the coastline in order to avoid crossing different coral communities.

104   Transects were randomly laid and all starting points were geo-referenced. Details of the sites are

105   given in Table 1. Surveys were conducted over two consecutive summers (December 2010 -

106   January 2012) and winters (September 2010 - October 2011) to gain a measure of seasonality in

107   the prevalence of PorBBD. Averaged sea surface temperatures ranged from 23.5°C in winter to

108   31.6°C in summer in Reunion. All massive *P. lutea* and *P. lobata* displaying signs of PorBBD

109   were counted along each transect. *P. lutea* is a common coral on Reunion Island coral reefs and is

110   mostly found on the reef flat (0.5-1.5 m deep). Colonies are generally brown, yellow-brown or

111   yellow green in colour with coralites filled with skeletal elements. In contrast, *P. lobata* is

112   relatively rare on the reef flat and commonly forms helmet-shaped colonies with lobed upper

113   surfaces. Colonies are mainly purple-blue and the coralites have relatively few skeletal elements

114 (Faure pers. comm.).The prevalence of PorBBD was estimated as = [(the number of PorBBD-

115 infected colonies)/ (the total number of massive *Porites* >2 cm) × 100], counted along each transect

116 in 1 m × 1 m quadrats (20-40 quadrats per transect). Finally, disease fronts were monitored on a

117 monthly basis from 30 November 2010 to 10 December 2011 in order to follow PorBBD

118 progression. Nails were driven into the dead portions of five *Porites lutea* colonies behind disease

119 front as reference markers for this purpose. The progression rate was recorded as the linear distance

120 between the nails and the nearest live tissue using photographs.

121 *Histopathology*

122 Samples of *Porites lutea* exhibiting signs of PorBBD were collected using SCUBA and

123 snorkelling. Core samples (10 mm core tubes) were taken from three healthy (HT) and five

124 diseased (DT) tissues, and fixed in 4% formalin for histological examination of their tissue

125 structure. Diseased tissue (DT) was sampled at the lesion boundary interface separating dead tissue

126 from healthy tissue (HT), while control tissue (CT) was cored from an apparently uninfected

127 colony. All DT, HT and CT samples were then coated in 1.5% (w/v) agarose to retain the spatial

128 integrity of the tissues. They were then decalcified using 1% HCl and EDTA renewed every 12 h

129 until process completion. Decalcified tissues were finally dehydrated in a gradient of ethanol baths,

130 cleared with xylene and embedded in paraffin wax. Cross sections of 6-8 μm thick were cut using

131 a microtome, mounted on glass slides and stained with Harris haematoxylin and eosin containing

132 phloxine B as previously described for the diagnosis of tissue fragmentation, necrosis and the

133 identification of invasive organisms (Sudek et al. 2012; Work & Aeby 2011). Serial sections were

134 examined under a light microscope and photographed using NIS Element software (Nikon©).

135 *Cyanobacterial culturing, isolation, and identification*

136   Fresh PorBBD mat was collected from four infected *Porites lutea* colonies using needles and

137   sterile syringes to identify the dominant cyanobacterial strains. Samples were placed in 10 ml

138   centrifuge tubes with seawater and held in darkness at 20°C until the return to the laboratory.

139   Cyanobacterial filaments (one when possible) were isolated from the raw samples under a light

140   microscope and transferred to agar plate containing Z8 medium (Kotai 1972) enriched with

141   NaHCO3, $(NH_4)_2SO_4$ and Vitamin B12. Inoculated plates were incubated at 27°C with a 12h

142   light:dark photoperiod and constant irradiance of 20 µmol photons m^{-2} s^{-1}. Bacterial strains were

143   routinely passaged between petri dishes in order to obtain clonal isolates for use in molecular

144   analysis. Genomic DNA was then extracted from each cyanobacterial isolate by boil lysing in 100

145   µL of 5mM Tris/HCl at 100°C for 5 minutes. PCR amplification was carried out in a volume of

146   25 µl GoTaq®Hot Start Green Master Mix (Promega, Madison, WI) containing 0.5mM of 16S

147   rRNA gene cyanobacterial primers CYA781R/CYA106F (Nübel et al. 1997; Rasoulouniriana et

148   al. 2009; Sussman et al. 2006) and 10 ng of template DNA. Amplification conditions for the PCR

149   included an initial denaturing step of 5 min at 94˚C, followed by 35 cycles at 94˚C for 60 sec, 60˚C

150   for 60 sec, 72˚C for 60 sec, and a final extension step of 5 min at 72˚C. Sequences obtained for

151   each cyanobacterial strain were examined for error and edited using GENEIOUS™ Pro (V.5.6.6)

152   sequencing software (Kearse et al. 2012). All consensus sequences were submitted to BLAST at

153   the National Centre for Biotechnology Information (NCBI, www.ncbi.nlm.nih.gov) and compared

154   with published sequences. The 16S rRNA sequences were aligned with reference sequences from

155   closely related to known cyanobacterial strains available in genbank. A phylogenetic tree was built

156   by neighbour-joining in GENEIOUS™ Pro (V.5.6.6) with bootstrap values based on 1000

157   replicates.

158   *Metagenomic profile of bacterial 16S rRNA genes*

159   Sample collection and DNA extraction

160   Samples of *Porites lutea* were collected from healthy (HT) and diseased (DT) sections of two

161   infected *P. lutea* colonies as well as a single control sample (CT). DT were sampled from the lesion

162   boundary interface with visually healthy tissue (HT), and the sample of CT was taken from

163   completely asymptomatic coral colonies. Cores of DT, HT and CT (2.2 cm diameter to a depth of

164   0.5-1 cm) were collected using a sterile stainless steel core tube and placed individually in sterile

165   disposable 50 ml polypropylene centrifuge tubes and kept under low light conditions at 2°C in a

166   cool box. Immediately upon return to the laboratory, the seawater within each tube was decanted

167   and the coral samples were immersed in absolute ethanol and stored at -80°C for molecular

168   analysis. To ensure that we had collected *P. lutea*, all samples were examined under the microscope

169   prior their preservation in absolute ethanol.

170   Bacterial genomic DNA was extracted from CT, HT and DT using the NucleoSpin® Soil Kit

171   (NucleoSpin Extract II, *Macherey-Nagel*, Düren, Germany). Approximately 150 mg of both tissue

172   and skeleton were scratched from the core surface using a sterile scalpel blade, placed in a 1.5 ml

173   centrifuge tube with 700 µl of lysis buffer and crushed using a fresh disposable plastic rod. Samples

174   were then placed in lysing matrix tubes for DNA extraction. The DNA was eluted with 50 µl sterile

175   elution buffer and its quality was verified by electrophoresis in agarose gels (1.5% wt/vol) stained

176   with GelRed™ (Biotium Inc., Hayward, California, USA).

177   PCR and 454 pyrosequencing

178   The composition of bacterial communities associated with CT, HT and DT samples was analysed

179   using 454-pyrosequencing technology (Roche, Nutley, NJ, USA) at GENOSCREEN (Campus de

180   l'Institut Pasteur de Lille, France). In our design, 16S rRNA variant regions V3 and V4 were

181   amplified   using   forward   (TACGGRAGGCAGCAG)   and   reverse

182   (GGACTACCAGGGTATCTAAT) primers. These primers were linked to 5' with MID tags, a

183   GsFLX key and GsFLX adapters. Each sample was amplified independently twice with distinct

184   MID tags, allowing the identification of each gene pool. Quality control was performed using the

185   Agilent DNA 100 (Agilent Technologies). The quantity of each PCR product was measured with

186   Picogreen and all products were mixed in equimolar concentrations prior to 454 GsFLX

187   sequencing.

188   Sequences analyses

189   All 454 GSFLX sequences were sorted by MID identification using GENEIOUS^{TM} Pro (V.5.6.3).

190   All generated reads were analysed using the SILVA online NGS tool (available online at www.arb-

191   silva.de/ngs). Raw sequence reads were aligned with a gap extension penalty of 2 and a gap penalty

192   of 5. Reads were filtered based on the following quality criteria: Minimum length - 200 bp,

193   minimum quality score - 30, maximum percent ambiguities - 1%, minimum base pair score - 30

194   and maximum percent repetitive - 2%. Remaining reads were clustered into operational taxonomic

195   units (OTUs) at a threshold sequence identity of 99%. OTUs were classified by BLAST score

196   comparison against the SILVA rRNA database version 115, with a classification similarity

197   threshold of 93%. Data from the SILVA classification were exported for further processing in

198   MEGAN software version 5.0.78 beta (Huson et al. 2007) using the lowest common ancestor

199   (LCA) algorithm with all parameters kept at default values (min support, 5; min score, 35; top

200   percent, 10.0; win score, 0.0). Cyanobacterial 16S rRNA gene sequences are accessible through

201   the NCBI GeneBank database under accession numbers KF957835-38. Raw 454-pyrosequencing

202   reads were submitted in Study (BioProject PRJNA231011) to the NCBI Sequence Read Archive

203   (SRA).

204 *Statistical analysis*

205   Prevalence of PorBBD was calculated per transect and for each site. Data were tested prior to

206   analysis for homoscedasticity (Levene's test) and normality of variance (Kolmogorov-Smirnov

207   and Lilliefors tests) and were then log transformed [$\log_{10}$ (X)] for analysis of variance (ANOVA).

208   Variations in the prevalence of PorBBD over the two survey years in the consecutive summers and

209   winters and across reef zones (reef slope vs. reef flat) were tested using Factorial ANOVA

210   (STATISTICA 8). Fisher tests were performed for *post hoc* multiple comparison. Rarefaction

211   curves were performed on bacterial populations associated with each tissue category. Principal

212   coordinate analysis (PCoA) and cluster analysis were performed using the Bray–Curtis similarity

213   coefficient to compare the bacterial community structures of the different tissue categories and the

214   Simpson's and Shannon's diversity indices were calculated. Finally comparisons of average values

215   of bacterial communities associated with different tissue categories were performed using the *t*-

216   test in STATISTICA. Before analysis, all OTU counts were normalized to avoid bias due to

217   differences in the number of sequences obtained from each sample (Mitra et al. 2009).

218   **3. Results**

219   *PorBBD prevalence and virulence*

220   A total of 3520 m^2 of reef and 5363 massive colonies of *Porites lutea* and *Porites lobata* were

221   surveyed between September 2010 and January 2012. PorBBD varied seasonally and between the

222   two geomorphologic reef zones. For instance, colonies of *Porites* exhibited significantly higher

223   PorBBD prevalence on the reef flat (ANOVA: $F = 1.18$, $p < 0.01$), affecting an average of 4.1 ±

224   2.0 % (mean ± SE) colonies compared to those observed at the deeper sites (0.2 ± 0.4; mean ± SE).

225   The percentage of infected colonies recorded on both the reef flat and reef slope was significantly

226   higher during summers than winters (ANOVA $_{\text{winter 1 vs. summer 1}}$: $F = 3.89$, p < 0.01; ANOVA $_{\text{winter}}$

227    $_{\text{2 vs. summer 2}}$: $F = 0.6$, p < 0.05). The rate of tissue mortality measured on five massive colonies of

228   *P. lutea* between 2011 and 2012 was 4.4 ± 0.12 (mean $\pm$ SE) mm day^{-1}. Among the monitored

229   colonies, two died approximately 13 months after the beginning of the study.

230

231   *Microscopic characterisation of PorBBD*

232   Comparison of cross sections of PorBBD-infected *P. lutea* colonies (Fig. 3A) revealed the

233   presence of three distinct tissue regions; the first one being the oldest area of infection comprising

234   dead and degraded tissue associated with cell debris, endophytic algae and other organisms such

235   as cyanobacteria and ciliates (Fig. 3C). The second region was characterised by a mat of

236   microorganisms, where filamentous cyanobacteria were clearly visible (Fig. 3C) perforating the

237   compromised and dead tissues (Fig. 3E and F). Finally, the discoloured portion of the tissue next

238   to the black band contained granular pigmented cells in both the epidermis and gastrodermis (Fig.

239   3B). Basophilic bodies resembling bacterial aggregates were also observed in this tissue region

240   and were regularly surrounded by the same granular cells.

241   *Identification of the dominant cyanobacterial strain*

242   Cyanobacterial strains isolated from four individual PorBBD-infected *Porites lutea* formed dense

243   clumps of brown filaments that were able to colonize an entire petri dish surface (75 cm^2 of Z8

244   solid medium) in a single week (Fig. 4A). The four strains were motile and appeared

245   morphologically similar with pointed, arrow-like calyptra (Fig. 4B). The isolates were genetically

246   similar to each other (>98 % identity) and phylogenetically affiliated to the cyanobacteria

247   *Pseudoscillatoria coralii* (FJ210722) and *Roseofilum reptotaenium* (HM048872) (Fig. 4C).

248   *Compararison of bacterial community structure* of DT, HT and CT

249   Following Roche 454-pyrosequencing, a total of 52 257, 38 778 and 21 309 sequence reads were

250   obtained from PorBBD infected tissue (DT1a-DT1b and DT2a-DT2b), apparently healthy tissue

251   (HT1a-HT1b and HT2a-HT2b) and healthy (control) tissue (CTa and CTb) respectively (Table 2).

252   The number of OTUs obtained for each sample categoy are summerised in Table 2.

253   Bacterial community structures from different tissue samples were compared with Cluster analysis

254   in MEGAN (V5.0.77) based on Bray-Curtis similarity matrices (Fig. 5A). Results revealed three

255   clearly separated groups; Cluster 1 grouping all DTs, Clusters 2 and 3 grouping HT and CT

256   samples (Fig. 5A). Rarefaction curves (Fig. 5 B) nearly paralleled the x axis for the majority of

257   samples, indicating that the overall bacterial diversity had likely been exhaustively characterized

258   within the bounds of amplicon bias. Bacterial diversity estimated with Simpson's and Shannon's

259   diversity indices showed that DT had higher bacterial diversity than both HT and CT (Table 2).

260   *Diversity of bacterial community associated with PorBBD*

261   Bacterial communities associated with PorBBD tissues were comprised of 8-14 different bacterial

262   classes, dominated by *γ-proteobacteria, α-proteobacteria, Bacteroidetes, δ-proteobacteria, ε-*

263   *proteobacteria, Firmicutes* and *Cyanobacteri*a (Fig. 6A). In DT1, the *α-proteobacteria* (34.5 %)

264   and *γ-proteobacteria* (32.36 %) were most commonly represented, followed by *Bacteroidetes*

265   (11.26 %), *δ-proteobacteria* (10.62 %), *Firmicutes* (4.1%), *ε-proteobacteria* (3.94 %), and

266   *Cyanobacteria* (0.3 %) classes. DT2 was dominated by *γ-proteobacteria* (60.0 %), *ε-*

267   *proteobacteria* (11.45 %), *Bacteroidetes* (9.04 %), *Firmicutes* (6.7 %), *δ-proteobacteria* (5.2 %),

268   *α-proteobacteria* (3.0 %) and *Cyanobacteria* (0.4 %) classes. At a higher taxonomic level of

269   MEGAN's cladogram, 48 to 118 genera were obtained from DT (Table 2) with the *α-*

270   *proteobacteria* and *γ-proteobacteria* classes exhibiting the highest diversity (Fig. 6B). The most

271   dominant genera observed in DT were *Vibrio* (13.5-33.9 %), *Desulfovibrio* (4.8-13.2 %),

272   *Alteromonas* (3.2-15.5 %), *Arcobacter* (4.8-12.1 %), *Glaciecola* (4.1-10.2 %), *Salinimonas* (2.1-

273   5.0 %), *Ruegeria* (0.3-5.5 %), *Algicola* (0.3-4.4 %) and *Oscillatoria* (0.3-0.6 %).

274

275   *Diversity of bacterial community associated with HT and CT*

276   Bacterial communities of HT and CT samples were almost exclusively dominated by the *γ-*

277   *proteobacteria* class, comprising 98.2%, 96.9% and 95.9% of the total OTUs, respectively (Fig.

278   6A). Additional OTUs attributed to *α-proteobacteria*, *δ-proteobacteria*, *Actinobacteria*, *β-*

279   *proteobacteria* and *ε-proteobacteria* were also found in common but at very low percentages. A

280   total of 19-29 genera were obtained from the HT samples including *Endozoicomonas* (76.7-96.5

281   %), *Vibrio* (0.27-18.7 %), *Photobacterium* (0.41-1.07 %), *Acinetobacter* (0.14-0.38 %) and

282   *Pseudomonas* (0.08-0.43 %). Finally, OTUs obtained from CT were mainly represented by

283   *Endozoicomonas* (59.0-63.4 %), *Vibrio* (30.8-31.1 %), *Photobacterium* (1.8-2.6%) *Acinetobacter*

284   (0.5%) and *Propionigenium* (0.2-0.3 %).

285   *Comparative analysis of bacterial communities associated with DT, HT and CT*

286   The average number of OTUs affiliated to bacterial genera in DT was significantly different from

287   those in HT (*t-test*: df= 2 p<0.0001) and CT (*t-test*: df= 2 p= 0.0001). No significant difference

288   was obtained between HT and CT (*t-test*: df= 2 p= 0.99). In total, 29 different bacterial genera

289   were found only in DT (Fig. 7), 28 genera were uniquely found in HT, and 19 genera could be

290   found in both DT and HT. Among OTUs obtained only from DT, the most represented bacterial

291   genera were *Glaciecola* (4.1-10.2 %), *Salinimonas* (2.1-5.0 %), *Amphritea* (1.0-1.6 %),

292   *Rhodobacter* (0.2-2.3 %), *Shimia* (0.4-1.5%) and *Oscillatoria* (0.3-0.6 %). Of note, the genus

293   *Ruegeria*, *Desulfovibrio*, *Arcobacter*, *Alteromonas*, *Aestuaribacter*, *Salinimonas* and *Algicola*

294   were highly represented in DT but were also found in common with HT and/or CT at very low

295   percentage. The full distribution of bacterial genera per tissue sample is depicted in Figure 7 and

296   Table S1.

298   **4. Discussion**

299   This study constitutes the first characterisation of an atypical form of BBD found on Reunion coral

300   reefs, *Porites* black band disease (PorBBD). Surveys conducted on two geomorphological reef

301   zones revealed spatial variability, with more infected colonies on the reef flat (0.5-1m) than the

302   reef slope (10-20 m). Similar patterns were previously reported in Florida Keys (Kuta &

303   Richardson 2002), the Republic of Maldives (Montano et al. 2012) and southern India (Thinesh et

304   al. 2009; Thinesh et al. 2011) where typical BBD is more abundant at shallow than deep sites. This

305   may be due to the proximity of the Reunion reef to the coastline (± 500 m wide), where it is

306   constantly exposed to high and increasing anthropogenic stress from sewage discharges, land-

307   based pollution and eutrophication with compounds such as nitrates, ammonium, and phosphate

308   (Chazottes et al. 2002; Naim 1993). Several studies suggest that nutrient enrichment, sewage

309   discharge and runoff may facilitate and increase disease outbreaks by enhancing the pathogen

310   virulence and/or impairing host resistance (Haapkylä et al. 2011; Rodriguez & Croquer 2008; Voss

311   & Richardson 2006).

312   Seasonal variations were also observed between 2010 and 2012: the average prevalence of

313   PorBBD recorded on the reef flat peaked in summer 2010 (8.7 ± 2.8%; mean ± SE), dropped in

314   winter 2011 (1.4 ± 1.0%; mean ± SE) and then increased again the following summer (7.7 ± 2.5%;

315   mean ± SE). These results are consistent with those previously found during BBD surveys on the

316   Great Barrier Reef in Australia (Boyett et al. 2007; Sato et al. 2009) and in Venezuela (Rodriguez

317   & Croquer 2008), the Red Sea (Zvuloni et al. 2009) and on Caribbean reefs (Edmunds 1991).

318   Seasonal fluctuations in BBD prevalence have been generally assumed to be driven by high light

319   intensities and summer sea temperatures, which may reduce host resistance or/and increase

320   pathogen virulence (Boyett et al. 2007; Edmunds 1991; Kuta & Richardson 2002; Richardson &

321   Kuta 2003; Rodriguez & Croquer 2008; Rützler et al. 1983; Sato et al. 2009; Sato et al. 2010).

322   Richardson and Kuta (2003) showed that the association of high light and elevated temperatures

323   promote the growth and progression of the cyanobacterium *Phormidium corallyticum* forming a

324   dense mat. This BBD bacterial mat favouring the growth of sulphate reducers (*e.g. Desulfovibrio*

325   species) and sulphide oxidizers (e.g. *Beggiatoa* species), generates anoxic conditions harmful to

326   adjacent coral tissues. However, the hot season (December to March) in Reunion is also associated

327   with heavy rainfall, high levels of ground water infiltration and surface water runoff, leading to an

328   increased level of pollutants such as pesticide, fertiliser, sewage from septic systems and waste

329   water in lagoon waters (Chazottes et al. 2002; Naim 1993).

330   Field monitoring performed on tagged colonies confirmed the virulence of PorBBD with a mean

331   tissue mortality rate reaching 4.4 ± 0.12 mm day^{-1} (mean $\pm$ SE). This progression rate is similar to

332   values previously reported on typical BBD infected scleractininan corals in the Florida Keys (Kuta

333   & Richardson 1997), Australia (Boyett et al. 2007; Sato et al. 2010), Indonesia (Haapkylä et al.

334   2009) and India (Borger & Steiner 2005; Thinesh et al. 2009). Importantly, PorBBD demonstrated

335   a high destructive potential for Reunion reefs with full mortality observed for 2 out of 5 colonies

336   monitored over a one-year period.

337   Cross sections performed on PorBBD-infected tissues showed cyanobacterial aggregates similar

338   to those previously observed in several studies of typical BBDs (Ainsworth et al. 2007; Barneah

339   et al. 2007; Bythell et al. 2002; Sato et al. 2009). The 16S sequences of cyanobacteria associated

340   with PorBBD were closely related to cyanobacteria previously identified as *Pseudoscillatoria*

341   *coralii* (Rasoulouniriana et al. 2009) and *Roseofilum reptotaenium* (Casamatta et al. 2012) isolated

342   on different coral hosts from the northern Red Sea and the Caribbean, as well as with cyanobacteria

343   isolated from BBD colonies in the central Great Barrier Reef (Sato et al. 2010). Interestingly, this

344   isolate, in contrast to cyanobacterial strains described in previous studies had unusually pointed

345   terminal cells, or "calyptra", suggesting the presence of a different cyanobacterial species

346   associated with PorBBD.

347   Microscopic analysis also revealed the presence of filamentous cyanobacteria in both dead and

348   compromised tissues. The ability of cyanobacteria to penetrate coral tissue has been demonstrated

349   to play an important role in typical BBD investigations (Ainsworth et al. 2007; Barneah et al. 2007;

350   Sato et al. 2010). For instance, recent studies have suggested that the calyptra may be involved in

351   tissue invasion (Ainsworth et al. 2007; Kramarsky-Winter et al. 2014), possibly via the secretion

352   of toxins or other compounds (Miller & Richardson 2012; Mydlarz et al. 2010; Whitton 2008).

353   The precise mechanisms of coral invasion by cyanobacteria are however unknown and require

354   further investigation.

355   Granular and pigmented cells were found in high densities in PorBBD-infected tissue of *P. lutea*.

356   They were found mainly in DT and have been proposed to result from an immune response

357   (Mydlarz et al. 2010; Palmer et al. 2008). Additionally, basophilic bodies resembling bacterial

358   aggregates similar to those observed in *Porites* white patch syndrome (Séré et al. 2013) were found

359   in the discoloured tissue adjacent to the bacterial mat but were not observed in HT. Thus, it is

360   possible that other bacteria may promote PorBBD by initiating a primary infection that impairs the

361   immune processes in corals and promoting progression of cyanobacteria (Miller et al. 2011).

362   However, no evidence of direct physical destruction resulting from these basophilic bodies could

363   be detected in our histological sections.

364   Bacterial community analysis via V3-V4, 16S metabarcoding suggested that the number of

365   bacterial taxa identified in this study was higher than in other metagenomic analyses of bacterial

366   communities associated with scleractinian corals (Littman et al. 2011; Wegley et al. 2007). While

367   HT and CT mostly contained *γ-proteobacteria*, DT yielded bacterial sequences from *γ-*

368   *proteobacteria* (47.9 ± 2.44 %; mean ± SE)*, α-proteobacteria* (19.3 ± 4.2 %; mean ± SE),

369   *Bacteroidetes* (10.5 ± 0.4 %; mean ± SE), *δ-proteobacteria* (8.2 ± 1.1 %; mean ± SE), *ε-*

370   *proteobacteria* (8.0 ± 1.6 %; mean ± SE)*, Firmicutes* (5.6 ± 0.7 %; mean ± SE) *and Cyanobacteri*a

371   (0.4 ± 0.2 %; mean ± SE). This result is not similar to patterns generally observed in other studies

372   that have characterised microbial communities from typical BBDs (Arotsker et al. 2009; Cooney

373   et al. 2002; Frias-Lopez et al. 2002; Sato et al. 2013; Sekar et al. 2006). For instance, *α-*

374   *proteobacteria* has been reported as the most represented and diverse class associated with BBD

375   affecting scleractinian corals in several distant locations (Arotsker et al. 2009; Barneah et al. 2007;

376   Miller & Richardson 2011; Sekar et al. 2006), whereas *γ-proteobacteria* was the dominant class

377   in PorBDD. In addition, *C*yanobacteria sequences represented 4 to 25% of characterized bacteria

378   from typical BBD lesions (Arotsker et al. 2009; Barneah et al. 2007; Sato et al. 2013; Sekar et al.

379   2006) while only 0.4-0.6% of bacterial sequences from PorBBD had cyanobacteria origins. This

380   is consistent with the PorBBD phenotype, which has a lighter band colour, compared to typical

381   thick dark BBD. However, our further use of analytic tools such as ProbeMatch (Kim et al. 2009)

382   suggests that these results should be interpreted with caution due to the inherent bias in taxon

383   identification by PCR amplification due to the affinity of the primers targeting the V3-V4 region.

384   Among the major classes found in this study, the *γ-proteobacteria Vibrio* was the dominant genus

385   in PorBBD-infected tissues representing 23.1 ± 2.1 % (mean ± SE) of the overall OTUs. Several

386   members of this genus have been identified as pathogens of corals, their virulence being attributed

387   to enzyme secretions that initiate tissue penetration and degradation (Ben-Haim & Rosenberg

388   2002; Ben-Haim et al. 2003; Rosenberg & Falkovitz 2004). This study revealed the presence of

389 OTUs attributed to *Vibrio* that are known to be highly proteolytic. However, since vibrionic OTUs

390 were also abundant in non-infected tissues, their role in PorBBD in *P. lutea* needs to be

391 individually assessed using multidisciplinary approaches combining bacterial culturing and

392 inoculation/infection trials (Henle-Koch's postulates).

393 The next most represented bacteria in PorBBD samples were *Desulfovibrio* and *Arcobacter*,

394 accounting for 8.6 ± 1.5 % (mean ± SE) and 7.9 ± 1.3 % (mean ± SE) of the overall OTUs,

395 respectively. These *Proteobacteria* have previously been found in BBD-infected corals from

396 different locations (Frias-Lopez et al. 2002; Sato et al. 2013) and seem to be important contributors

397 to BBD aetiology, producing sulfated compounds suspected to exacerbate microbial virulence

398 (Sato et al. 2009). Although a very low percentage of these sulfide-reducing bacteria was found in

399 healthy tissues, their relatively high abundance in PorBBD tissues suggests a tropism towards

400 anoxic micro-environments (Cooney et al. 2002; Glas et al. 2012; Sato et al. 2010; Sekar et al.

401 2008; Sekar et al. 2006; Viehman et al. 2006) rich in carbon compounds derived from cell debris

402 and other organic nutrients produced during coral tissue lysis (Viehman et al. 2006). Other

403 predominant genera affiliated to *Glaciecola*, *Salinimonas*, *Amphritea*, and *Shimia* were recorded

404 only in PorBBD-infected corals but have not been reported in typical BBDs. Interestingly, *Shimia*

405 was recently associated with a newly-reported *Porites* white patch syndrome on western Indian

406 Ocean reefs (Séré et al. 2013), however no evidence of its pathogenicity has been established in

407 this study. Importantly, no OTUs affiliated to potential pathogenic bacteria including *Cytophaga*,

408 *Clostridium*, *and Campylobacter*, which generally occur in typical BBDs (Cooney et al. 2002;

409 Frias-Lopez et al. 2004; Frias-Lopez et al. 2002; Sato et al. 2013; Sato et al. 2010) lesions were

410 retrieved in PorBBD samples. Finally, no sulfide-oxydizing *Beggiatoa* related OTUs were

411 retrieved from diseased samples while they have been commonly reported in typical BBDs (Sekar

412 et al. 2008), but this again may be explained by the bias introduced by amplifying primer

413 sequences, primer mismatches or limiting DNA template concentrations that have previously been

414 reported to impair PCR (Frias-Lopez et al. 2002; Sekar et al. 2006).

415 In summary, the importance of PorBBD for Indian Ocean coral reefs should not be underestimated

416 due to its potential for rapid progression in slowly growing reef-building corals and the associated

417 high mortality rate. This disease shows several similarities with classical BBD manifestations, for

418 example, the spatial and temporal patterns and propagation of PorBBD seem to be in agreement

419 with those influencing typical BBDs. Moreover, cyanobacterial filaments in PorBBD are

420 genetically closely related to those identified elsewhere. However, PorBBD exhibits key features

421 that differ from typical BBD manifestations: Firstly, an apparent low level of cyanobacterial

422 infection produces a sparse black band, which is preceded by a discoloured tissue region.

423 Basophilic bodies resembling bacterial aggregates were found in the discoloured tissue region,

424 suggestive of an independent primary infection. Finally, an atypical composition of the associated

425 bacterial communities suggests differing aetiology of PorBBD. However the presence of sulfate-

426 reducers or sulfide-oxidizers, previously shown to be associated with an anoxic microenvironment

427 within typical BBD, confirms that PorBBD is a manifestation of BBD. Further investigations,

428 towards infection trials, would be required to elucidate the complex interactions between *Porites*

429 associated microbial communities and identify potential pathogenic candidates by fulfilling

430 Koch's postulates.

431

432 **Acknowledgements**: We greatly thank Dr. Jean Turquet and Yann Gomard (CRVOI) for their

433 help and guidance in the laboratory. Finally, we would like to address a special thanks to our

434   colleague and great friend Stephanie Bollard (ARVAM). This study would not have been the same

435   without her generous assistance, advice and valuable support.

436

437

References

Aeby GS, and Santavy DL. 2006. Factors affecting susceptibility of the coral *Montastraea faveolata* to black-band disease. *Marine Ecology-Progress Series* 318:103-110.

Ainsworth TD, Kramasky-Winter E, Loya Y, Hoegh-Guldberg O, and Fine M. 2007. Coral Disease Diagnostics: What's between a plague and a band? *Applied and Environmental Microbiology* 73:981-992.

Al-Moghrabi S. 2001. Unusual black band disease (BBD) outbreak in the northern tip of the Gulf of Aqaba (Jordan). *Coral Reefs* 19:330-331.

Antonius A. 1981. The 'band' diseases in coral reefs. *Proceedings of the Forth International Coral Reef Symposium*. p 7-14.

Arotsker L, Siboni N, Ben-Dov E, Kramarsky-Winter E, Loya Y, and Kushmaro A. 2009. *Vibrio* sp. as a potentially important member of the Black Band Disease (BBD) consortium in *Favia* sp. corals. *FEMS Microbiology Ecology* 70:515-524.

Barneah O, Ben-Dov E, Kramarsky-Winter E, and Kushmaro A. 2007. Characterization of black band disease in Red Sea stony corals. *Environmental Microbiology* 9:1995-2006.

Ben-Haim Y, and Rosenberg E. 2002. A novel *Vibrio* sp. pathogen of the coral *Pocillopora damicornis*. *Marine Biology* 141:47-55.

Ben-Haim Y, Thompson FL, Thompson CC, Cnockaert MC, Hoste B, Swings J, and Rosenberg E. 2003. *Vibrio coralliilyticus* sp. nov., a temperature-dependent pathogen of the coral *Pocillopora damicornis*. *International Journal of Systematic Evolutionary Microbiology* 53:309-315.

Borger JL, and Steiner SC. 2005. The spatial and temporal dynamics of coral diseases in Dominica, West Indies. *Bulletin of Marine Science* 77:137-154.

Boyett HV. 2006. The ecology and microbiology of black band disease and brown band syndrome on the Great Barrier Reef. Master's thesis. James Cook University, Townsville.

Boyett HV, Bourne DG, and Willis BL. 2007. Elevated temperature and light enhance progression and spread of black band disease on staghorn corals of the Great Barrier Reef. *Marine Biology* 151:1711-1720.

Bythell J, Barer M, Cooney R, Guest J, O'Donnell A, Pantos O, and Le Tissier M. 2002. Histopathological methods for the investigation of microbial communities associated with disease lesions in reef corals. *Letters in applied microbiology* 34:359-364.

Casamatta D, Stanic D, Gantar M, and Richardson LL. 2012. Characterization of *Roseofilum reptotaenium* (Oscillatoriales, Cyanobacteria) gen. et sp. nov. isolated from Caribbean black band disease. *Phycologia* 51:489-499.

Chazottes V, Le Campion-Alsumard T, Peyrot-Clausade M, and Cuet P. 2002. The effects of eutrophication-related alterations to coral reef communities on agents and rates of bioerosion (Reunion Island, Indian Ocean). *Coral Reefs* 21:375-390. 10.1007/s00338-002-0259-0

Cooney R, Pantos O, Le Tissier M, Barer M, O'Donnell A, and Bythell J. 2002. Characterization of the bacterial consortium associated with black band disease in coral using molecular microbiological techniques. *Environmental Microbiology* 4:401-413.

Dinsdale E. 2002. Abundance of black-band disease on corals from one location on the Great Barrier Reef: a comparison with abundance in the Caribbean region. *Proceedings of the Ninth International Coral Reef Symposium*, Bali, 23–27 October 2000. p 1239-1243.

Edmunds PJ. 1991. Extent and effect of black band disease on a Caribbean reef. *Coral Reefs* 10:161-165.

Frias-Lopez J, Klaus JS, Bonheyo GT, and Fouke BW. 2004. Bacterial community associated with black band disease in corals. *Applied and Environmental Microbiology* 70:5955-5962.

Frias-Lopez J, Zerkle AL, Bonheyo GT, and Fouke BW. 2002. Partitioning of bacterial communities between seawater and sealthy, black band diseased, and dead coral surfaces. *Applied and Environmental Microbiology* 68:2214-2228. 10.1128/aem.68.5.2214-2228.2002

486   Gantar M, Kaczmarsky LT, Stanić D, Miller AW, and Richardson LL. 2011. Antibacterial activity of
487   marine and black band disease cyanobacteria against coral-associated bacteria. *Marine Drugs*
488   9:2089-2105.
489   Garrett P, and Ducklow H. 1975. Coral diseases in Bermuda. *Nature* 253:349-350.
490   Glas MS, Sato Y, Ulstrup KE, and Bourne DG. 2012. Biogeochemical conditions determine virulence of
491   black band disease in corals. *The ISME Journal* 6:1526-1534.
492   Haapkylä J, Unsworth RK, Flavell M, Bourne DG, Schaffelke B, and Willis BL. 2011. Seasonal rainfall
493   and runoff promote coral disease on an inshore reef. *PLoS ONE* 6:e16893.
494   Haapkylä J, Unsworth RKF, Seymour AS, Melbourne-Thomas J, Flavell M, Willis BL, and Smith DJ. 2009.
495   Spatio-temporal coral disease dynamics in the Wakatobi Marine National Park, South-East
496   Sulawesi, Indonesia. *Diseases of Aquatic Organisms* 87:105-115.
497   Huson DH, Auch AF, Qi J, and Schuster SC. 2007. MEGAN analysis of metagenomic data. *Genome*
498   *Research* 17:377-386.
499   Kearse M, Moir R, Wilson A, Stones-Havas S, Cheung M, Sturrock S, Buxton S, Cooper A, Markowitz S,
500   and Duran C. 2012. Geneious Basic: an integrated and extendable desktop software platform for the
501   organization and analysis of sequence data. *Bioinformatics* 28:1647-1649.
502   Kim YJ, Teletia N, Ruotti V, Maher CA, Chinnaiyan AM, Stewart R, Thomson JA, and Patel JM. 2009.
503   ProbeMatch: rapid alignment of oligonucleotides to genome allowing both gaps and mismatches.
504   *Bioinformatics* 25:1424-1425.
505   Kotai J. 1972. Instructions for preparation of modified nutrient solution Z8 for algae. *Norwegian Institute*
506   *for Water Research, Oslo* 11:5.
507   Kramarsky-Winter E, Arotsker L, Ras7ulouniriana D, Siboni N, Loya Y, and Kushmaro A. 2014. The
508   possible role of cyanobacterial filaments in coral black band disease pathology. *Microbiol Ecology*
509   67:177-185. 10.1007/s00248-013-0309-x
510   Kuta K, and Richardson L. 1997. Black band disease and the fate of diseased coral colonies in the Florida
511   Keys. *Proceedings of the Eighth International Coral Reef Symposium*. p 575-578.
512   Kuta K, and Richardson L. 2002. Ecological aspects of black band disease of corals: relationships between
513   disease incidence and environmental factors. *Coral Reefs* 21:393-398.
514   Littman R, Willis BL, and Bourne DG. 2011. Metagenomic analysis of the coral holobiont during a natural
515   bleaching event on the Great Barrier Reef. *Environmental Microbiology* 3:651-660.
516   Miller AW, Blackwelder P, Al-Sayegh H, and Richardson LL. 2011. Fine-structural analysis of black band
517   disease-infected coral reveals boring cyanobacteria and novel bacteria. *Diseases of Aquatic*
518   *Organisms* 93:179-190.
519   Miller AW, and Richardson LL. 2011. A meta-analysis of 16S rRNA gene clone libraries from the
520   polymicrobial black band disease of corals. *FEMS Microbiology Ecology* 75:231-241.
521   Miller AW, and Richardson LL. 2012. Fine structure analysis of black band disease (BBD) infected coral
522   and coral exposed to the BBD toxins microcystin and sulfide. *Journal of Invertebrate Pathology*
523   109:27-33.
524   Mitra S, Klar B, and Huson DH. 2009. Visual and statistical comparison of metagenomes. *Bioinformatics*
525   25:1849-1855.
526   Montano S, Strona G, Seveso D, and Galli P. 2012. First report of coral diseases in the Republic of
527   Maldives. *Diseases of Aquatic Organisms* 101:159-165.
528   Mydlarz LD, McGinty ES, and Harvell CD. 2010. What are the physiological and immunological responses
529   of coral to climate warming and disease? *Journal of Experimental Biology* 213:934-945.
530   Myers JL, and Richardson LL. 2009. Adaptation of cyanobacteria to the sulfide-rich microenvironment of
531   black band disease of coral. *FEMS Microbiology Ecology* 67:242-251.
532   Myers JL, Sekar R, and Richardson LL. 2007. Molecular detection and ecological significance of the
533   cyanobacterial genera *Geitlerinema* and *Leptolyngbya* in black band disease of corals. *Applied and*
534   *Environmental Microbiology* 73:5173-5182.
535   Naim O. 1993. Seasonal responses of a fringing-reef community to eutrophication (Reunion-Island,
536   Western Indian-Ocean). *Marine Ecology-Progress Series* 99:137-151.

537   Nübel U, Garcia-Pichel F, and Muyzer G. 1997. PCR primers to amplify 16S rRNA genes from
538   cyanobacteria. *Applied and Environmental Microbiology* 63:3327-3332.
539   Palmer CV, Mydlarz LD, and Willis BL. 2008. Evidence of an inflammatory-like response in non-normally
540   pigmented tissues of two scleractinian corals. *Proceedings of the Royal Society B: Biological*
541   *Sciences* 275:2687-2693.
542   Rasouloniriana D, Siboni N, Ben-Dov E, Kramarsky-Winter E, Loya Y, and Kushmaro A. 2009.
543   *Pseudoscillatoria coralii* gen. nov., sp, nov., a cyanobacterium associated with coral black band
544   disease (BBD). *Diseases of Aquatic Organisms* 87:91.
545   Raymundo L, and Weil E. 2016. Indo-Pacific coloured band diseases of corals. In: CM Woodley CD, AW
546   Bruckner, JW Porter, SB Galloway, ed. *Diseases of Corals*: Wiley Blackwell, pp. 333-344.
547   Richardson LL. 2004. Black band disease. *Coral Health and Disease*: Springer, 325-336.
548   Richardson LL, and Kuta KG. 2003. Ecological physiology of the black band disease cyanobacterium
549   *Phormidium corallyticum*. *FEMS Microbiology Ecology* 43:287-298.
550   Richardson LL, Miller AW, Broderick E, Kaczmarsky L, Gantar M, and Sekar R. 2009. Sulfide,
551   microcystin, and the etiology of black band disease. *Diseases of Aquatic Organisms* 87:79.
552   Rodriguez S, and Croquer A. 2008. Dynamics of Black Band Disease in a *Diploria strigosa* population
553   subjected to annual upwelling on the northeastern coast of Venezuela. *Coral Reefs* 27:381-388.
554   Rosenberg E, and Falkovitz L. 2004. The *Vibrio shiloi*/*Oculina patagonica* model system of coral
555   bleaching. *Annual Review Microbiology* 58:143-159.
556   Rützler K, Santavy DL, and Antonius A. 1983. The black band disease of Atlantic reef corals. 111.
557   Distribution, ecology, and development. *Marine Ecology* 4:329-358.
558   Sato Y, Bourne DG, and Willis BL. 2009. Dynamics of seasonal outbreaks of black band disease in an
559   assemblage of *Montipora* species at Pelorus Island (Great Barrier Reef, Australia). *Proceedings of*
560   *the Royal Society B: Biological Sciences* 276:2795-2803.
561   Sato Y, Willis B, and Bourne D. 2013. Pyrosequencing-based profiling of archaeal and bacterial 16S rRNA
562   genes identifies a novel archaeon associated with black band disease in corals. *Environmental*
563   *Microbiology* 15:2994-3007.
564   Sato Y, Willis BL, and Bourne DG. 2010. Successional changes in bacterial communities during the
565   development of black band disease on the reef coral, *Montipora hispida*. *The ISME Journal* 4:203-
566   214.
567   Sekar R, Kaczmarsky LT, and Richardson LL. 2008. Microbial community composition of black band
568   disease on the coral host *Siderastrea siderea* from three regions of the wider Caribbean. *Marine*
569   *Ecology-Progress Series* 362:85-98.
570   Sekar R, Mills DK, Remily ER, Voss JD, and Richardson LL. 2006. Microbial communities in the surface
571   mucopolysaccharide layer and the black band microbial mat of black band-diseased *Siderastrea*
572   *siderea*. *Appled and Environmental Microbiology* 72:5963-5973. 10.1128/aem.00843-06
573   Séré MG, Chabanet P, Turquet J, Quod J-P, and Schleyer MH. 2015. Identification and prevalence of coral
574   diseases on three Western Indian Ocean coral reefs. *Diseases of Aquatic Organisms* 114:249-261.
575   Séré MG, Tortosa P, Chabanet P, Turquet J, Quod J-P, and Schleyer MH. 2013. Bacterial communities
576   associated with *Porites* white patch syndrome (PWPS) on three Western Indian Ocean (WIO) coral
577   reefs. *PLoS ONE* 8:e83746.
578   Sudek M, Work T, Aeby G, and Davy S. 2012. Histological observations in the Hawaiian reef coral, *Porites*
579   *compressa*, affected by *Porites* bleaching with tissue loss. *Journal of Invertebrate Pathology*
580   111:121-125.
581   Sussman M, Bourne DG, and Willis BL. 2006. A single cyanobacterial ribotype is associated with both red
582   and black bands on diseased corals from Palau. *Diseases of Aquatic Organisms* 69:111-118.
583   Sutherland KP, Porter JW, and Torres C. 2004. Disease and immunity in Caribbean and Indo-Pacific
584   zooxanthellate corals. *Marine Ecology-Progress Series* 266:265-272.
585   Thinesh T, Mathews G, and Edward J. 2009. Coral disease prevalence in Mandapam group of islands, Gulf
586   of Mannar, Southeastern India. *Indian Journal of Marine Sciences* 38:444-450.

587 Thinesh T, Mathews G, and Patterson Edward J. 2011. Coral disease prevalence in the Palk Bay,
588   Southeastern India—With special emphasis to black band. *Indian Journal of Marine Sciences*
589   40:813.
590 Viehman S, Mills D, Meichel G, and Richardson L. 2006. Culture and identification of *Desulfovibrio* spp.
591   from corals infected by black band disease on Dominican and Florida Keys reefs. *Diseases of*
592   *Aquatic Organisms* 69:119-127.
593 Voss JD, Mills DK, Myers JL, Remily ER, and Richardson LL. 2007. Black band disease microbial
594   community variation on corals in three regions of the wider Caribbean. *Microbiol Ecology* 54:730-
595   739.
596 Voss JD, and Richardson LL. 2006. Nutrient enrichment enhances black band disease progression in corals.
597   *Coral Reefs* 25:569-576.
598 Wegley L, Edwards R, Rodriguez-Brito B, Liu H, and Rohwer F. 2007. Metagenomic analysis of the
599   microbial community associated with the coral *Porites astreoides*. *Environmental Microbiology*
600   9:2707-2719.
601 Whitton BA. 2008. Cyanobacterial diversity in relation to the environment. *Algal toxins: Nature,*
602   *occurrence, effect and detection*: Springer, 17-43.
603 Work TM, and Aeby GS. 2006. Systematically describing gross lesions in corals. *Diseases of Aquatic*
604   *Organisms* 70:155-160. 10.3354/dao070155
605 Work TM, and Aeby GS. 2011. Pathology of tissue loss (white syndrome) in *Acropora* sp. corals from the
606   Central Pacific. *Journal of Invertebrate Pathology* 107:127-131.
607 Zvuloni A, Artzy-Randrup Y, Stone L, Kramarsky-Winter E, Barkan R, and Loya Y. 2009. Spatio-temporal
608   transmission patterns of black-band disease in a coral community. *PLoS ONE* 4:e4993.

609

610

611   **List of figures**

612   Fig. 1. Map showing the study sites in Reunion Island, Western Indian Ocean.

613   Fig. 2. Massive colonies of *Porites lutea* exhibiting signs of *Porites* black band disease (PorBBD)

614   at A) Ravine des Poux, B) and C) La Corne, and D) Trou d'Eau in Reunion Island. Ds = dead

615   skeleton; Bcy = black cyanobacteria; Wf = white front; Ht = healthy tissue.

616   Fig. 3. Histological sections of *Porites lutea*: A) Healthy tissue (Ht). Note the integrity of the

617   epidermis. B) Living polyp from PorBBD-infected tissue (Dt) showing high concentration of

618   granular pigmented cells (pc). Note the basophilic bodies (bb) surrounded by granular pigmented

619   cells. C) Degraded tissue with cell debris (cd) and residual pigmented cells (pc). Note the presence

620   of ciliate-like organisms (ci). D) Disease (Dt) band boundary characterised by a dense mat of

621   filamentous cyanobacteria (cy) invading the fragmented tissue (ft). E) and F) penetration of

622   filamentous cyanobacteria (white arrow) into the infected tissue (Dt).

623   Fig. 4. Cyanobacteria retrieved from *Porites* black band disease (PorBBD): A**)** Clumps of brown

624   cyanobacterial filaments (cy) growing in a petri dish with Z8 medium. B**)** Photomicrograph of

625   the cyanobacterial strain CYPBD1, closely related to the cyanobacterium *Pseudoscillatoria coralii*

626   (FJ210722) and *Roseofilum reptotaenium* (HM048872), isolated from pure cultures. Note the

627   pointed terminal calls called calyptra (cal). C) Neighbour-joining phylogenetic tree showing the

628   relatedness of the strains CPPORBBD1, CPPORBBD2, CPPORBBD3, and CPPORBBD4 with

629   reference *cyanobacterial* strains. Numbers at each node are bootstraps values (%) obtained after

630   1000 iterations.

631   Fig. 5. Comparative analysis of bacterial communities associated with three tissue categories of

632   *Porites lutea*. A) Cluster diagram and B) rarefaction curves of bacterial communities associated

633   with HT1-2 = healthy tissue, CT = control tissue and DT 1-2 = diseased tissue of *Porites lutea*,

634   created using MEGAN software version 5.0.78 beta. Numerals a and b distinguish the duplicate

635   samples.

636   Fig. 6. Bacterial community structures based on the classification of partial 16S RNA genes

637   obtained from *Porites* black band disease lesions and healthy colonies of *Porites lutea* using

638   MEGAN. A) Relative abundance (%) of bacterial classes and B) number of bacterial genera

639   assigned to the diverse classes associated with PorBBD-infected tissues (DT1 and DT2), healthy

640   tissues (HT1 and HT2) and control tissue (CT). Numerals a and b distinguish the duplicate

641   samples.

642   Fig. 7. Venn diagram of bacterial genera showing their distributions in PorBBD-infected tissues

643   (DT), healthy tissues (HT) and control tissue (CT). * indicates potentially pathogenic bacterial

644   genera as identified in a literature survey of coral disease.

645

Study sites in Reunion Island

Map showing the study sites in Reunion Island, Western Indian Ocean.
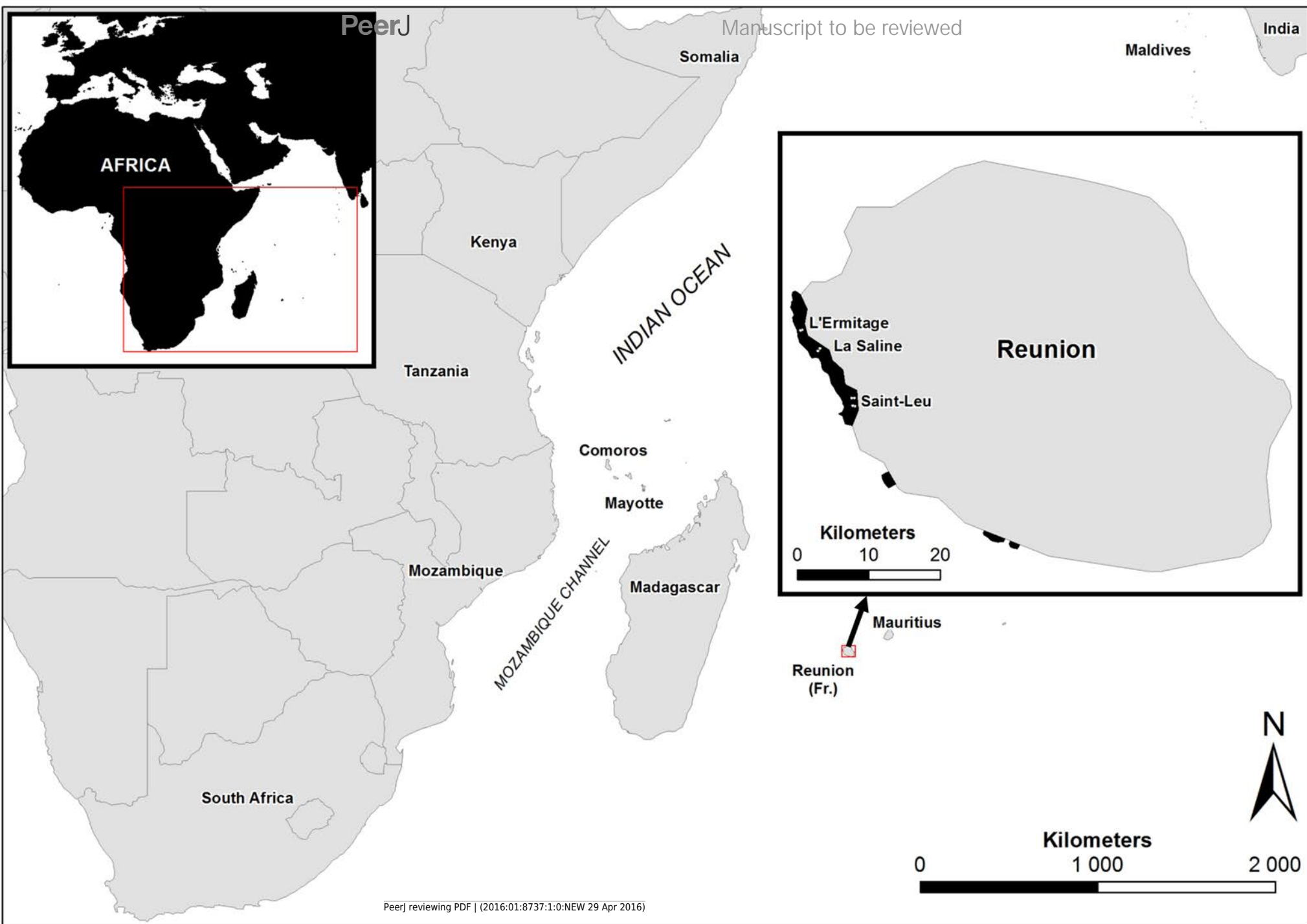
Massive colonies of *Porites lutea* exhibiting signs of *Porites* black band disease (PorBBD) at
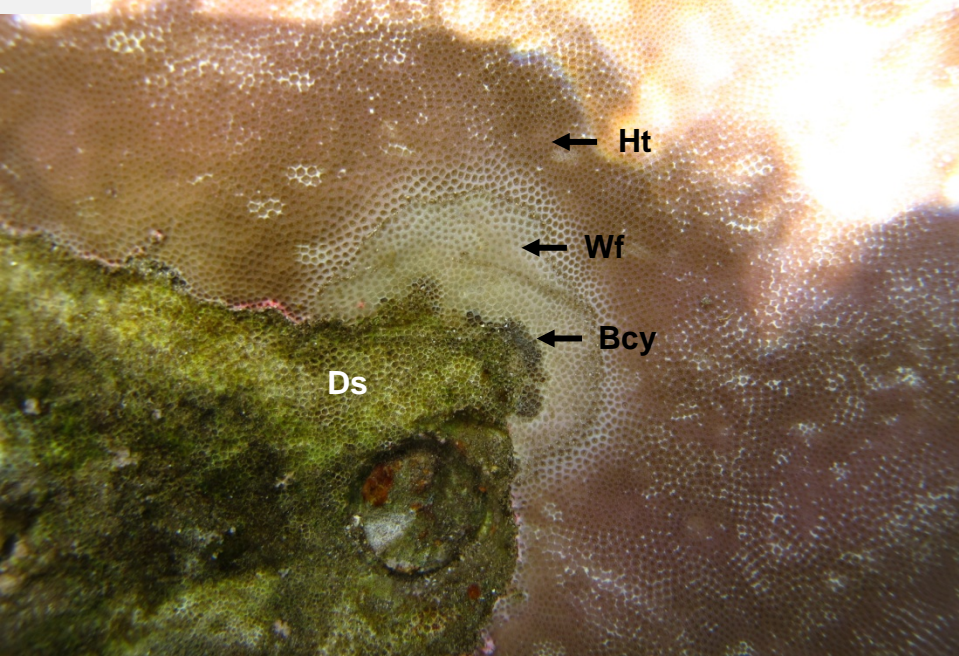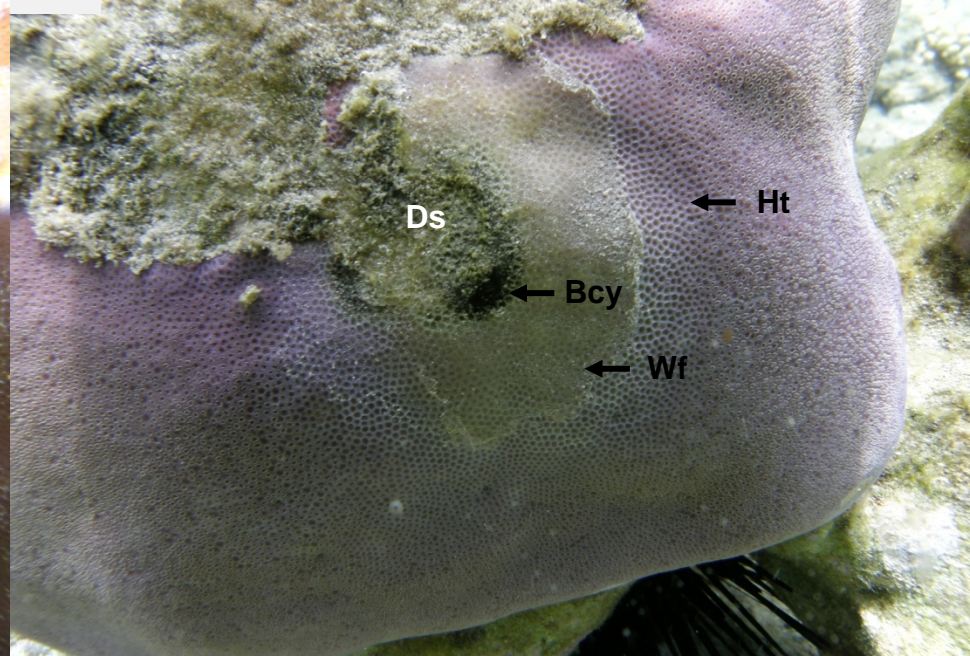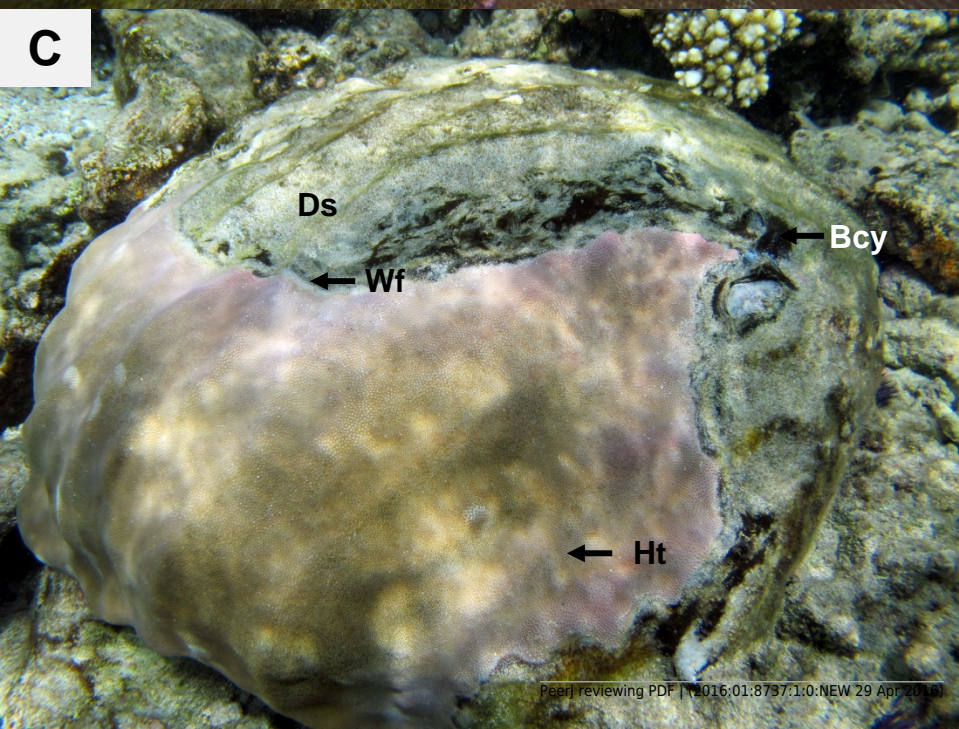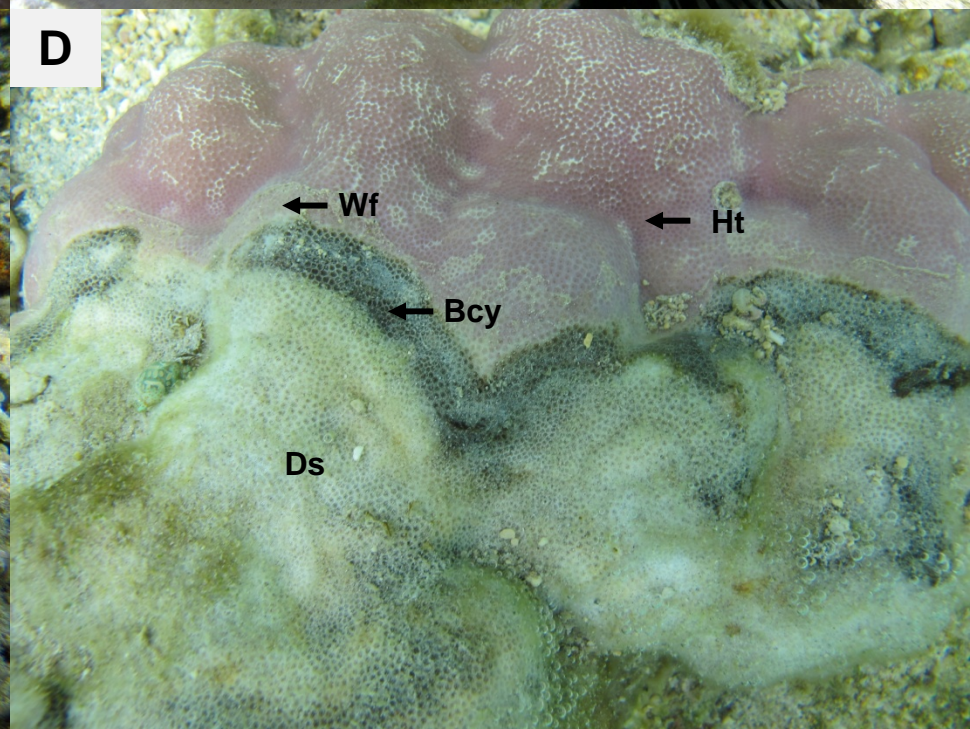
A) Ravine des Poux, B) and C) La Corne, and D) Trou d'Eau in Reunion Island. Ds = dead skeleton; Bcy = black cyanobacteria; Wf = white front; Ht = healthy tissue.

Histological sections of *Porites lutea*:
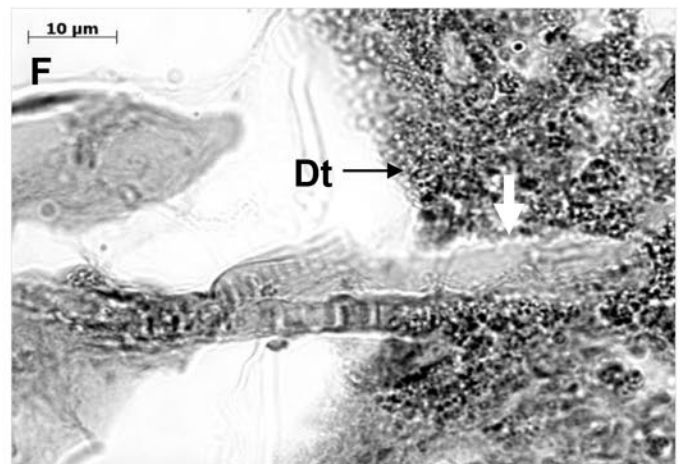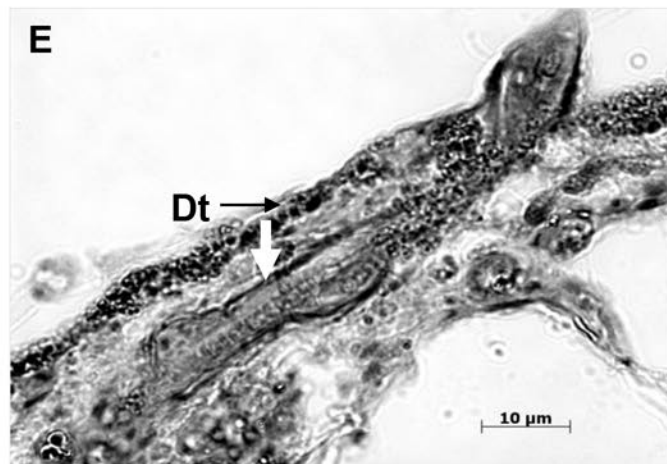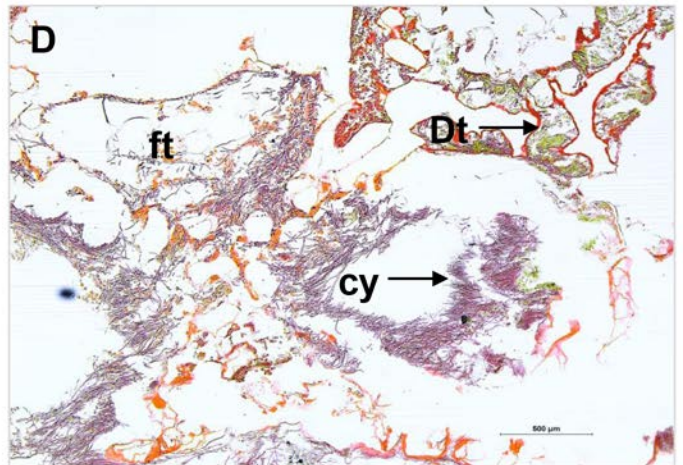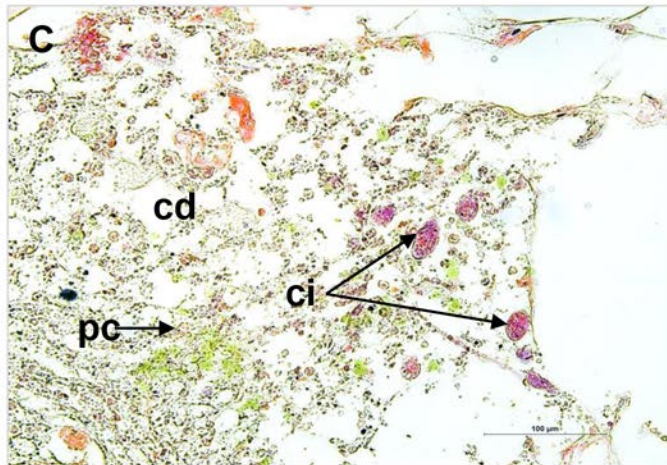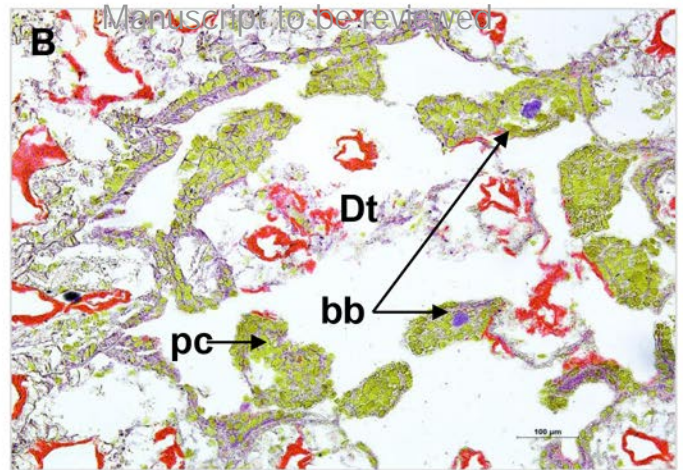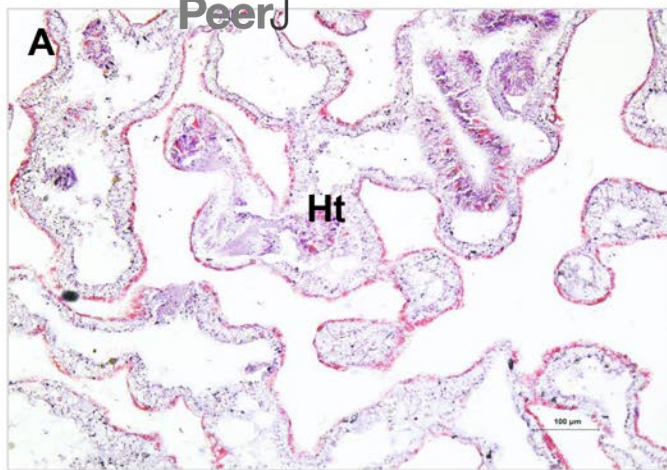
A) Ravine des Poux, B) and C) La Corne, and D) Trou d'Eau in Reunion Island. Ds = dead skeleton; Bcy = black cyanobacteria; Wf = white front; Ht = healthy tissue.

Cyanobacteria retrieved from *Porites* black band disease (PorBBD):

A) Clumps of brown cyanobacterial filamments (cy) growing in a petri dish with Z8 medium.
B) Photomicrograph of the cyanobacterial strain CYPBD1, closely related to the
cyanobacterium *Pseudoscillatoria coralii* (FJ210722) and *Roseofilum reptotaenium*
(HM048872), isolated from pure cultures. Note the pointed terminal calls called calyptra (cal).
C) Neighbour-joining phylogenetic tree showing the relatedness of the strains CPPORBBD1,
CPPORBBD2, CPPORBBD3, and CPPORBBD4 with reference *cyanobacterial* strains. Numbers
at each node are bootstraps values (%) obtained after 1000 iterations.

A
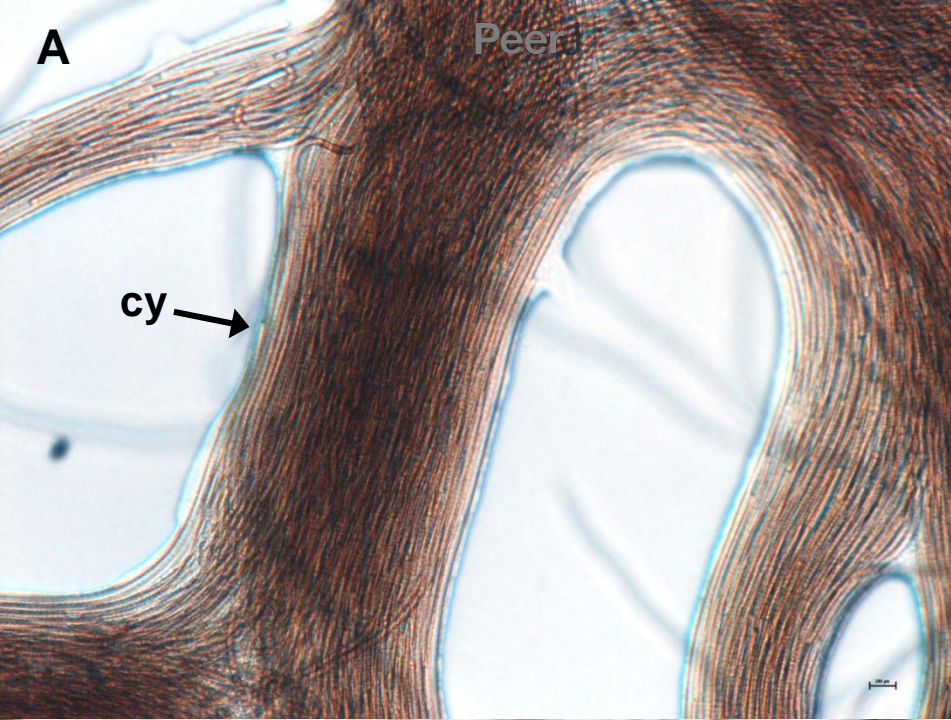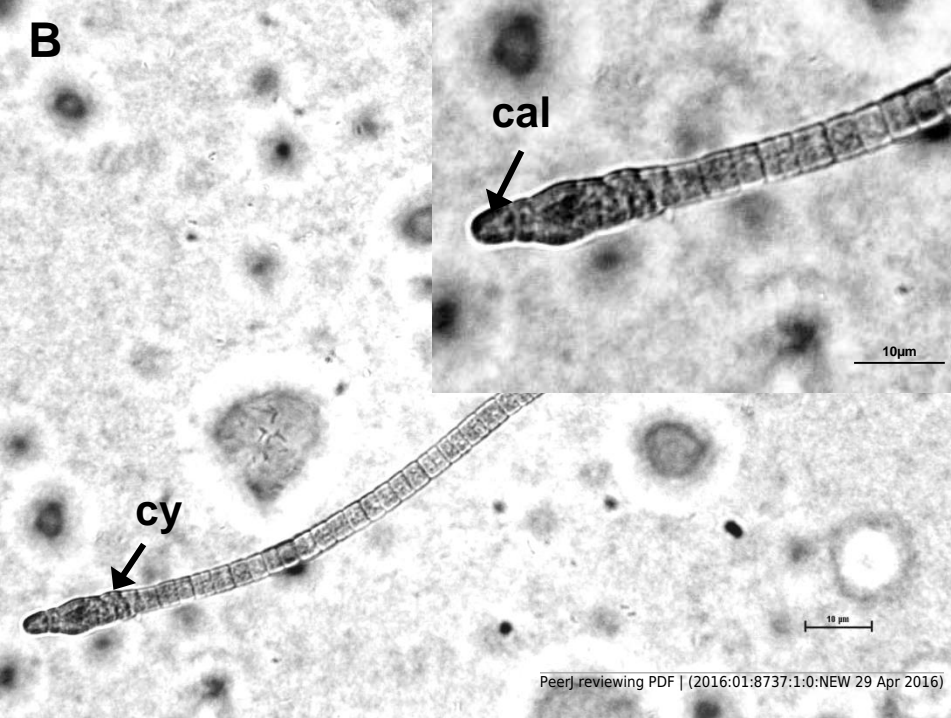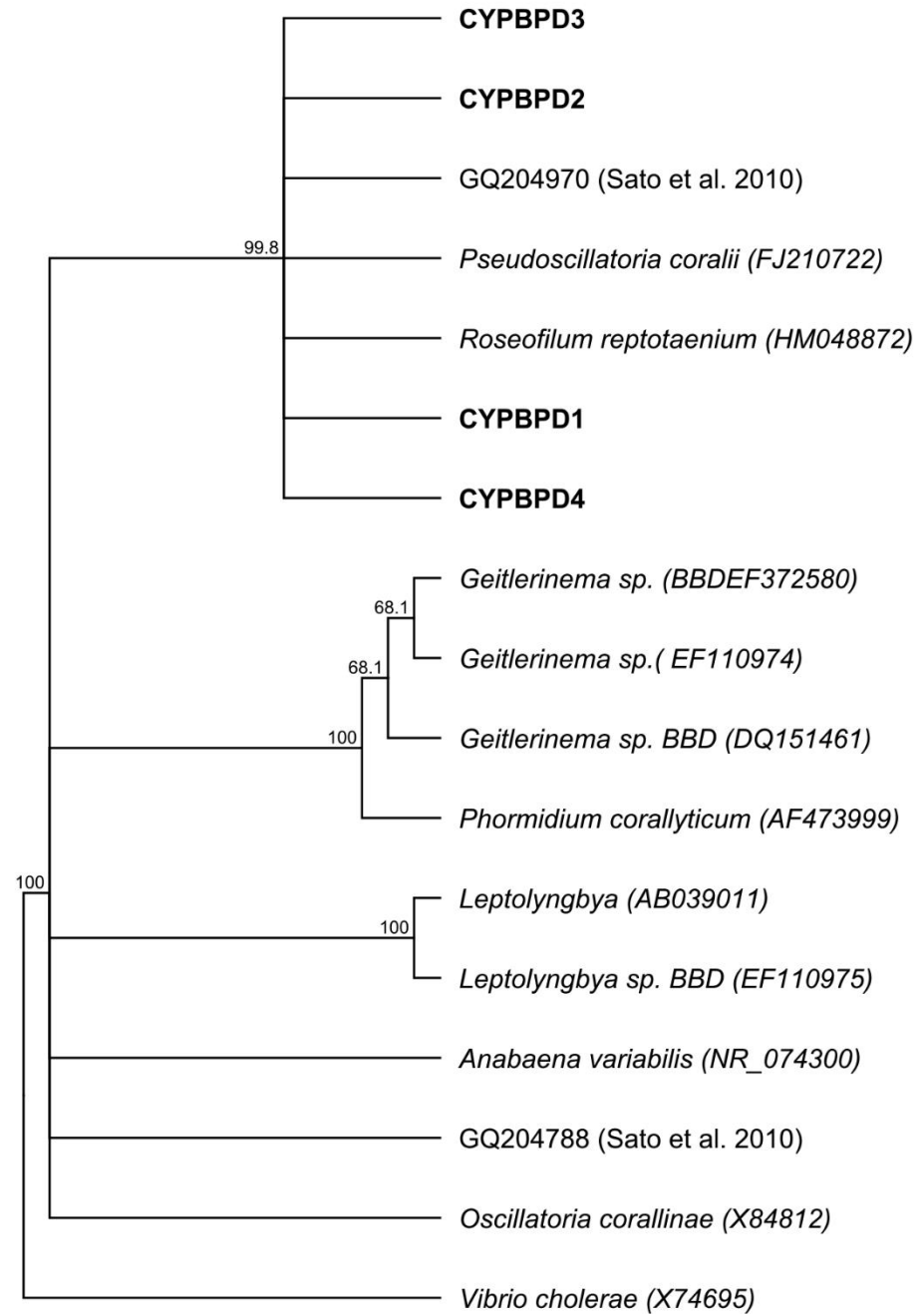
B

cal

cy

cy

CYPBPD3

CYPBPD2

GQ204970 (Sato et al. 2010)

Pseudoscillatoria coralii (FJ210722)

99.8

Roseofilum reptotaenium (HM048872)

CYPBPD1

CYPBPD4

Geitlerinema sp. (BBDEF372580)

68.1

Geitlerinema sp.(EF110974)

68.1

Geitlerinema sp. BBD (DQ151461)

100

Phormidium corallyticum (AF473999)

Leptolyngbya (AB039011)

100

Leptolyngbya sp. BBD (EF110975)

100

Anabaena variabilis (NR_074300)

100

GQ204788 (Sato et al. 2010)

Oscillatoria corallinae (X84812)

Vibrio cholerae (X74695)

Bacterial community structures based on the classification of partial 16S RNA genes obtained from Porites black band disease lesions and healthy colonies of Porites lutea using MEGAN

A) Relative abundance (%) of bacterial classes and B) number of bacterial genera assigned to the diverse classes associated with PorBBD-infected tissues (DT1 and DT2), healthy tissues (HT1 and HT2) and control tissue (CT). Numerals a and b distinguish the duplicate samples.

1
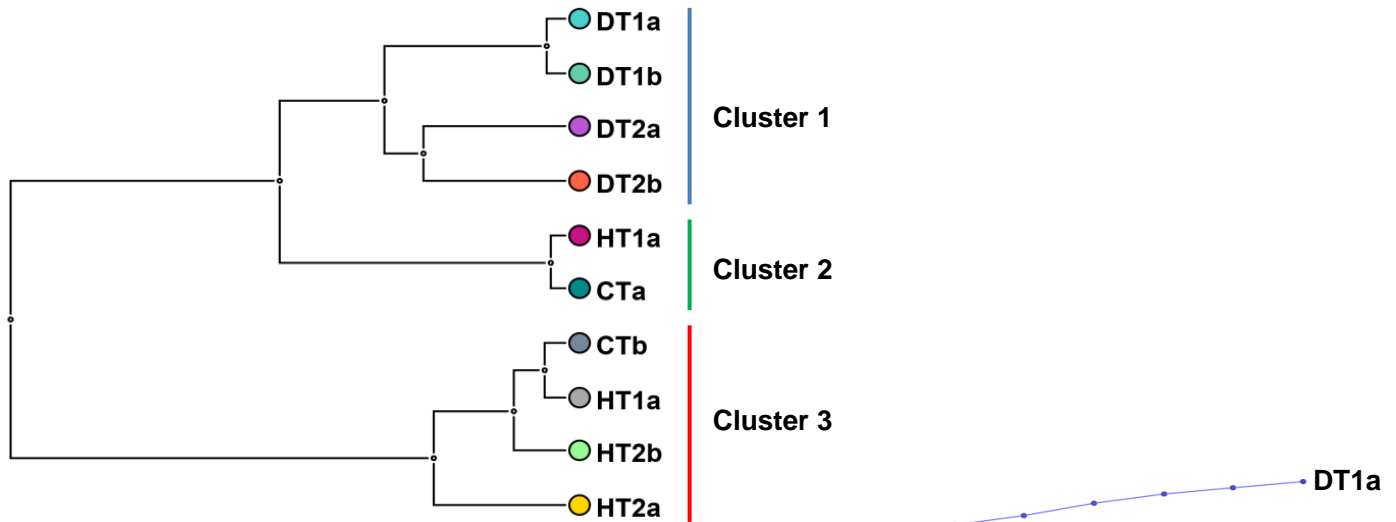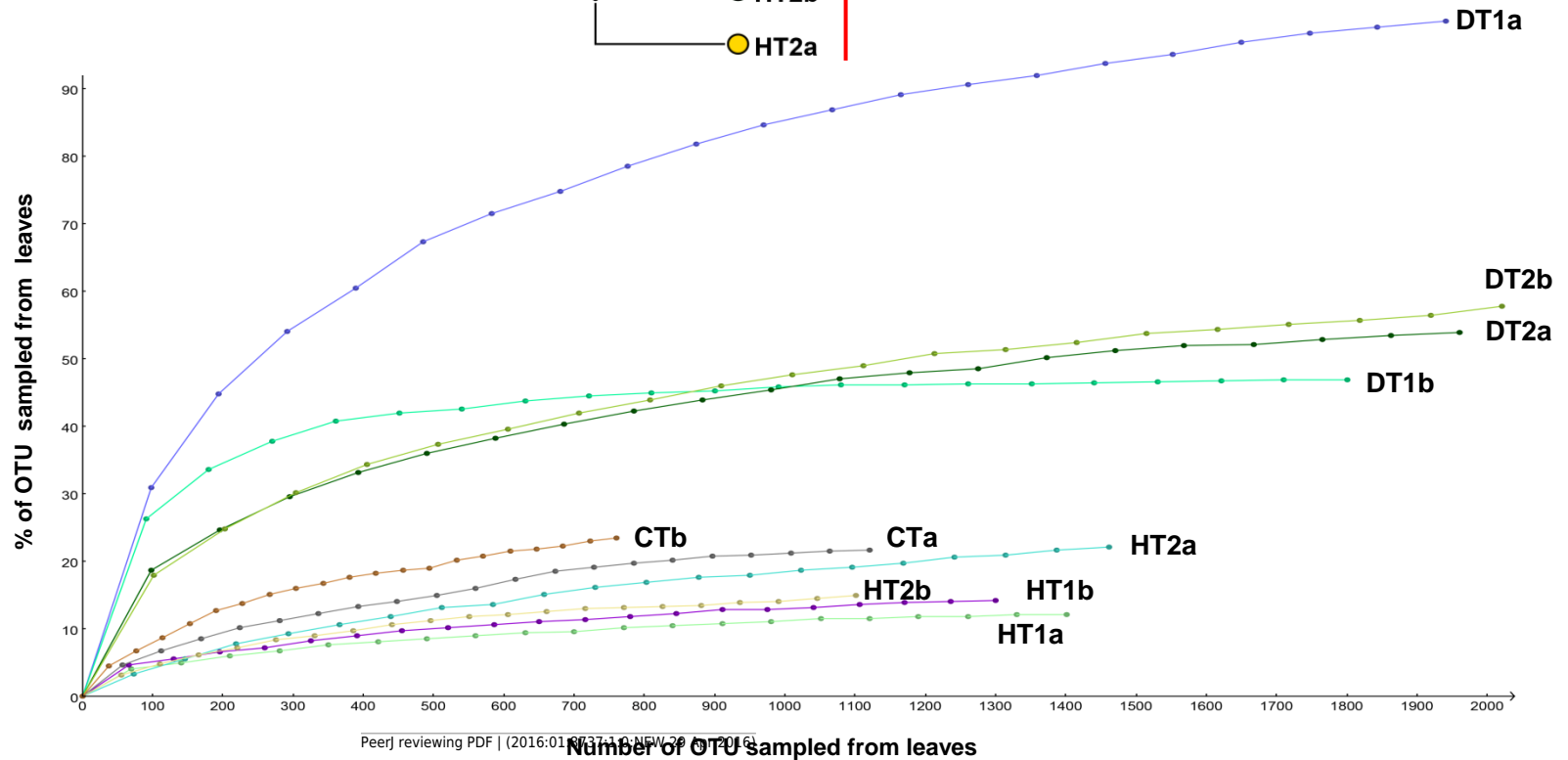
Comparative analysis of bacterial communities associated with three tissue categories of *Porites lutea*.

A) Cluster diagram and B) rarefaction curves of bacterial communities associated with HT1-2 = healthy tissue, CT = control tissue and DT 1-2 = diseased tissue of *Porites lutea*, created using MEGAN software version 5.0.78 beta. Numerals a and b distinguish the duplicate samples.

1low
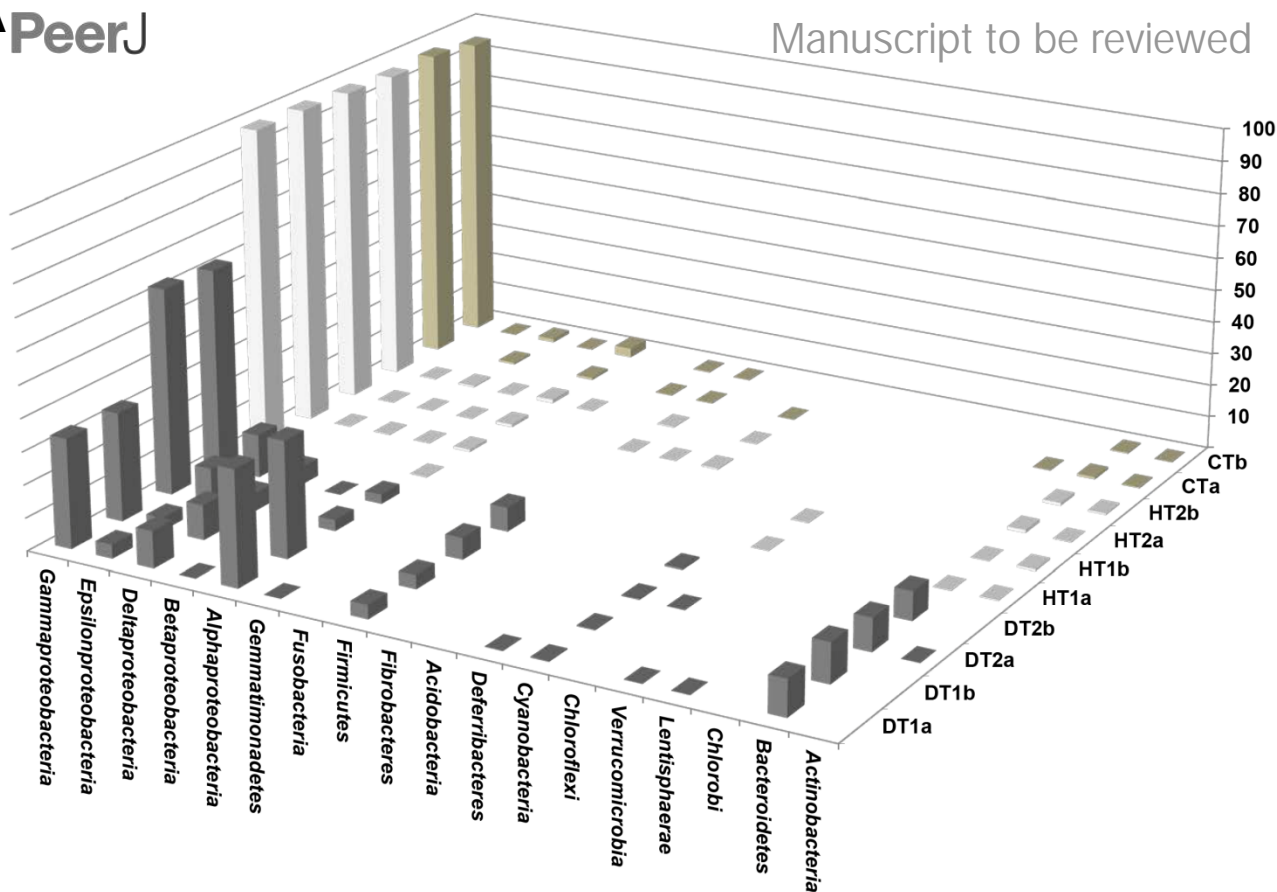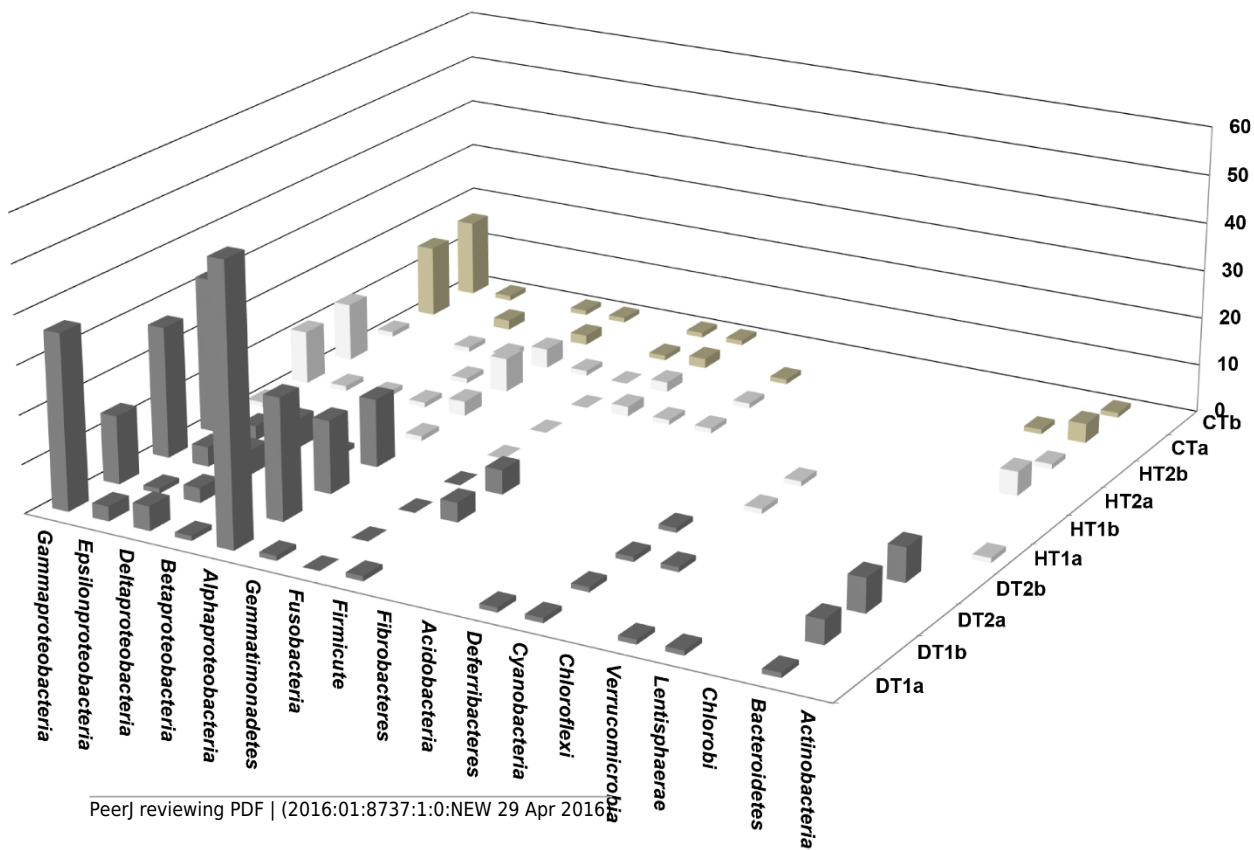
Venn diagram of bacterial genera showing their distributions in:

PorBBD-infected tissues (DT), healthy tissues (HT) and control tissue (CT). * indicates

potentially pathogenic bacterial genera as identified in a literature survey of coral diseases.

Disease tissue (DT)

Control tissue (CT)

Flexithrix
*Lachnospiraceae**
Nitratireductor
Labrenzia
Phaeobacter
Rhodobacter
Roseobacter
*Roseovarius**
*Shimia**
Tateyamaria
Thalassobacter
Thalassococcus
Gemmobacter
Sulfurospirillum
*Oscillatoria**

Glaciecola
Haliea
Marinobacterium
Salinimonas
Colwellia
*Escherichia**
Amphritea
Neptunomonas
Oceanobacter
Oceanospirillum
Oleiphilus
SUP05 cluster
*Enterovibrio**
Oceanicaulis

*Paracoccus**
Marinoscillum
Peredibacter
*Arcobacter**
Neptuniibacter
BD1-7 clade
Ruegeria

Ralstonia
Chloroflexi
Bradyrhizobium
Aliivibrio

Thalassospira
*Pseudoalteromonas**
Alteromonas
*Thalassomonas**
Algicola
Pseudomonas
Catenococcus
*Photobacterium**
*Vibrio**

Rhodobium
Pelagibius
Maricurvus
Endozoicomonas
Acinetobacter
Holophagae

Marinovum
*Desulfovibrio**
Aestuariibacter

Propionigenium
Segetibacter
Portibacter
Sunxiuqinia
Chloroherpeton
Lactobacillus
Peptostreptococcaceae
Maritimibacter
Acetobacteraceae
*Serratia**

Marinovum
Sphingobium
Sphingomonas
Massilia
Paramoritella
Thiohalocapsa

Healthy tissue (HT)

Location and depth of the reef sites and stations selected for this study.

1 **Table 1**: Location and depth of the reef sites and stations selected for this study.

Sites	Stations	Habitat	Reef depth (m)	Latitude/ longitude
L'Ermitage	3-Chameaux	Reef flat	0.5-1.0	-21.080351° ; 55.219576°
La Saline	Trou d'Eau	Reef flat	0.5-1.0	-21.103312° ; 55.242294°
Saint-Leu	La Corne	Reef flat	0.5-1.0	-21.165960° ; 55.285080°
Saint-Leu	Ravine des Poux	Reef flat	0.5-1.0	-21.176397° ; 55.285985°
L'Ermitage	3-Chameaux	Reef slope	10.0-12.0	-21.081281° ; 55.217590°
La Saline	Trou d'Eau	Reef slope	10.0-12.0	-21.106160° ; 55.239540°
Saint-Leu	La Corne	Reef slope	10.0-12.0	-21.165940° ; 55.281930°
Saint-Leu	Ravine des Poux	Reef slope	10.0-12.0	-21.175490° ; 55.283460°

Total sequences read before and after sequence trimming, number of bacterial classes and genera and diversity indices for each sample and subsample of PorBBD (DT1a-DT1b and DT2a-DT2b), apparently healthy tissue (HT1a-HT1b and HT2a-HT2b) and control tissue

1   **Table 2**: Total sequences read before and after sequence trimming, number of bacterial classes and genera

2   and diversity indices for each sample and subsample of PorBBD (DT1a-DT1b and DT2a-DT2b), apparently

3   healthy tissue (HT1a-HT1b and HT2a-HT2b) and control tissue (CTa and CTb).

	DT1a	DT1b	DT2a	DT2b	HT1a	HT1b	HT2a	HT2b	CTa	CTb
Σ raw sequences	11 320	12 703	14 848	13 386	15 660	14 646	19 008	15 221	12 563	8746
Σ OTU	2560	2569	2338	2363	1417	1334	1484	1149	1160	801
Σ bacterial Phylum	14	8	12	10	6	8	13	12	14	11
Σ genera	118	48	63	69	15	19	29	22	29	32
Shannon index	4.689	4.586	4.477	4.509	3.333	3.398	3.204	3.191	3.563	3.666
Simpson reciprocal index	13.642	13.334	13.458	13.650	9.090	9.294	8.336	8.326	9.949	10.215